Title	Digital simulation of dominant eddies of a co-flowing jet
Author(s)	Lai, CCK; Lee, JHW; Lam, KM
Citation	The 16th IAHR-APD 2008 Congress and 3rd Symposium of IAHR-ISHS, Nanjing, China, 20-23 October 2008. In Advances in Water Resources & Hydraulic Engineering, 2009, v. 2, p. 618-623
Issued Date	2009
URL	http://hdl.handle.net/10722/133499
Rights	Creative Commons: Attribution 3.0 Hong Kong License

DIGITAL SIMULATION OF DOMINANT EDDIES OF A CO-FLOWING JET

Chris C.K. Lai①, Joseph H.W. Lee②, K.M. Lam③

① MPhil Candidate, The University of Hong Kong, Hong Kong, China, chris812@graduate.hku.hk
② Professor, The University of Hong Kong, Hong Kong, China, hreclhw@hkucc.hku.hk
③ Associate Professor, The University of Hong Kong, Hong Kong, China, kmlam@hku.hk

Abstract This paper described a method for virtual construction of turbulent jet flow field from a limited set of experimental data. The objective is for jet visualization enhancement in near-field plume models. The method is based on the proper orthogonal decomposition (POD), which is an efficient tool to capture the turbulent field based on principal components. A set of experimental flow images at a number of cross-sections of a coflowing jet is obtained in the laboratory. Four hundred instantaneous flow images are taken at each jet section and are subjected to POD analysis. The first 60 principal modes are used in the reconstruction of jet turbulence via a low dimensional generation of jet images. The inclusion of additional modes is shown to produce little improvement on the visual appearance of the reconstructed jet images. Linear interpolation is attempted to generate jet images at an intermediate jet section between two experimental stations. Jet flow field on a central longitudinal section of the jet are assembled from the reconstructed flow images at all jet sections. The resulting development of concentration jet width is shown to agree well with the analytical solution.

Key words proper orthogonal decomposition (POD); jet visualization; integral model

1 INTRODUCTION

Many plume models commonly used today (e.g. Visual Plume, USEPA - Baumgartner et al.1994) solve the Navier-Stokes equations for turbulent shear flows via an integral approach that has simplified the computation effort enormously and yet produces accurate results. The integral model is far less computational demanding than the solution of Reynolds Averaged Navier-Stokes equations with turbulence closure models. However, the turbulent components of the flow are not readily obtained from the integral models and only average jet trajectories with smooth boundaries are provided. Some models simulate jet turbulence by stochastic methods but they do not give satisfactory results. In this paper, the proper orthogonal decomposition (POD) together with a database of experimental flow images obtained from laboratory is applied for the “virtual” reconstruction of flow turbulence in jet visualizations.

POD is an established method to produce low dimensional representations of experiment data and has been applied to turbulent jet flows (e.g., Bernero and Fiedler 2000). It is used extensively in studying coherent structures/ dominant eddies in boundary-layer type flows (e.g., Glauser et al. 1987). The essence of the method is that it captures satisfactorily the bulk of turbulence field with only a small number of principal mode shapes, in the order of 10, out of hundreds. This promotes computer memory saving; requires much less computation time and is thus advantageous in jet visualizations. The work described in this paper was the first step to investigate the applicability of POD in the virtual construction of turbulent jet images of a co-flowing momentum jet. Visualizations of jet flow by this method require input of laboratory data of which

instantaneous flow images in a number of jet cross-sections were captured with a laser-induced fluorescence (LIF). A brief description of the procedures involved is described in the following sections.

2 EXPERIMENTS AND ANALYSIS

The experiments were carried out in the Croucher Laboratory of Environmental Hydraulics at the University of Hong Kong. A 4.5m by 11m shallow water basin was filled with water to a depth of 30cm. A main flow stream was formed in the basin by re-circulating water with a pumping system. Two screens were installed at the basin inlet and outlet to enhance the uniformity of the flow stream and to reduce the ambient turbulence that would otherwise affect the experiment results. In this study, the ambient velocity was set constant at 5.2cm/s for all experiments. A homogenous solution of fluorescence dye and water was discharged into the basin horizontally from a circular nozzle of diameter D = 1cm, forming a coflowing jet. Laser induced fluorescence (LIF) was employed to measure dye concentration distributions at five downstream (x) locations. The fluorescent dye Rhodamine-6G (Rho-6G, $C_{28}H_{31}N_2O_3Cl$) was used. A laser beam from a 5-W Argon-ion laser was reflected by two properly aligned mirrors to a rotating mirror, producing a laser sheet. Under the excitation of laser light, the dye produced luminescence and LIF images of the jet section were captured by a camera. The image system consisted of a CCD camera and a computer with image capturing software installed. A CCD camera fitted with Nikkor 35mm lens was enclosed in a watertight Perspex casing and placed under water to view the jet sections from downstream. An orange filter was used to filter off the noise of the image. The software Global Lab Image 2 was used to capture the 8-bit image (with 255 grey levels) at a resolution of 576×768 pixels. The time delay between each image was set at 100 ms and 400 images were captured at each vertical cross-section.

Background concentration was subtracted from each instantaneous LIF image, after which the time-averaged concentration field was removed, leaving behind the fluctuating component of concentration field due to jet turbulence. POD analysis was then applied to the time sequence of LIF images to extract the principal mode shapes at each jet section. An analysis was carried out to determine the minimum number of modes needed to represent (reconstruct) the fluctuating concentration field satisfactorily at a measurement station of the jet. Jet images at an intermediate jet section were obtained by linear interpolation of the principal modes at two experimental stations bounding the particular jet section with the consideration of time lag. The time lag was found from the correlation matrix of the jet images at the two measurement stations. If jet visualizations are required on a longitudinal plane, the fluctuating concentration information at successive jet sections on that plane is aligned to produce the longitudinal images of the co-flowing jet.

3 RESULTS AND DISCUSSION

3.1 PRINCIPLE MODES AND INTERPOLATION

With an ensemble of 400 LIF images at each jet section, up to 400 POD modes can be computed. Fig. 1 shows the first six principal modes for the measurement stations at x/D = 10, 20, 30, 40 and 60. As the jet spreads downstream, the jet section becomes larger and jet width increases. In Fig. 1, the spatial scales of the modes at different x stations are non-dimensionalized by division with the concentration jet width, b_{gc}. It is found that the patterns of the modes do not change significantly (except for getting larger because of entrainment) as they move downstream. Each mode exhibits the same number of concentration maxima and minima at each jet section. This suggests that linear interpolation of jet images between any two adjacent sections is viable because the mechanism of turbulent entrainment

remains similar within the region bounded by them.

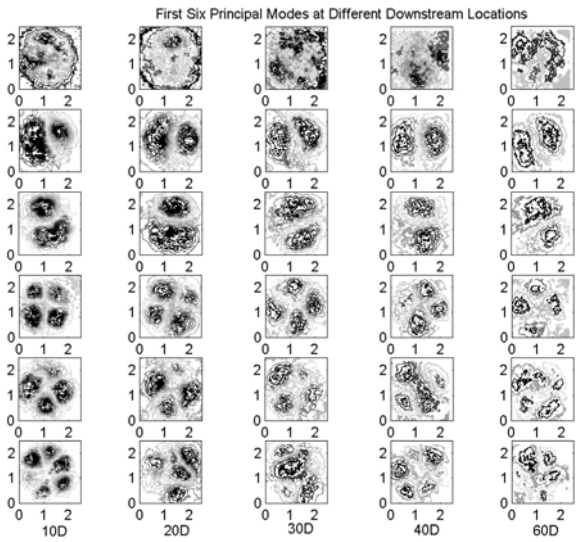

Fig. 1 First six principal modes at different downstream locations

The contribution of each POD mode to the total energy or variance of the turbulence field are shown in Fig. 2(a). The energy does not bear any physical meaning. It only represents the contribution of that mode to the total turbulence field (i.e. ensemble data). It is found that the energy contribution decreases rapidly with increasing mode number, indicating negligible contribution of the higher modes to the total turbulence field. The integral of the curve in Fig. 2(a) is shown in Fig. 2(b), and it measures the average amount of energy that is captured as function of number of modes included. The curves level off at about 30 modes. This suggests that flow information, on average, is captured sufficiently well by the first 30 modes and inclusion of higher modes has negligible improvement on both reconstruction and approximation Take the first six modes in Fig. 1 as an example, they together accounted for 42 % of the total variance at x = 10D. Fig. 2(b) shows that their combined energy increases with downstream distance, indicating that the gross behavior of the jet can be represented by a small number of modes. It is noted that the form and structures of these lower modes remain essentially unchanged when the ensemble size is changed to 100, 200, 300 or 400. This indicates that the principal modes can be well determined by a relatively small population of LIF images and the turbulence field is actually characterized by dominant eddies that are grossly independent to the ensemble size.

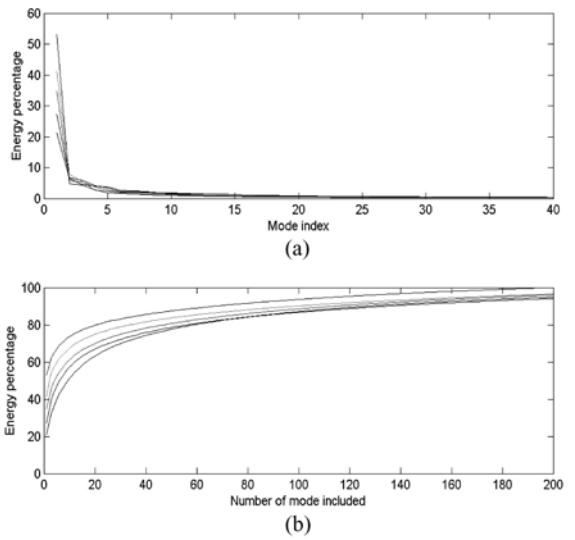

Fig. 2 Energy contribution of POD modes
(a) individual modes; (b) cumulative contribution

3.2 LOW DIMENSIONAL REPRESENTATION OF TURBULENCE FIELD

It is necessary to outline briefly the Karhunen-Loeve (K-L) procedure for POD analysis (Holmes et al. 1999). An ensemble member is defined as $\phi_k = \varphi_k - \overline{\varphi}$ and $\overline{\varphi} = \frac{1}{K}\sum_{k=1}^{K}\varphi_k$, where φ_k is the raw image. The K-L basis of orthonormal eigenfunctions is denoted by m^k and the corresponding eigenvalues by λ_k. It may be shown that the K-L basis is optimal in the sense that of all orthonormal bases, it gives the best approximation to ϕ_k on average for any specified number of terms. We can write $\phi_k = \sum_{k=1}^{N}\frac{a_k}{\lambda_k}m^k$ with the coefficient a_k defined as the inner product, $a_k = \int m^k \phi_k$ .The terms a_k are non-zero and they vary randomly, with the understanding that each a_k fluctuates about its own mean. The mean decreases with increasing mode number, that is, mode one has the largest mean. Due to the randomness of a_k, $\frac{a_k}{\lambda_k}$ can be treated as random coefficients and they

vary within the range of (−1,1). To compare the apparent "likeness" between reconstructed images and the instantaneous images, the mean square error is used and it is defined as $\varepsilon_n = \| \phi - \phi_k \|^2 / \| \phi \|^2$, where || || denotes inner product.

3.2.1 RECONSTRUCTION AND APPROXIMATION

By reconstruction, we mean the fitting of a member of the ensemble to the orthonormal basis whereas approximation means the projection of a flow image onto the basis, with understanding that it was not a member of the ensemble. First, we demonstrate two reconstruction examples of flow images. The first example is at the measurement station $x = 10D$. An instantaneous LIF image and its reconstruction using different numbers of modes are depicted in Fig. 3(a). It is evident that 60 modes are sufficient to capture the gross structure of the flow. The associated error defined by the eigenvalues is about 15%. With 100 modes, the error is down to 10%. This accuracy is expected since full reconstruction using all modes will be exact. For the second example at the station $x = 30D$, the reconstruction of a flow image is shown in Fig. 3(b). Most turbulent features of the flow can be captured by the first 40 modes with an error of 15%. The reduction in error is modest when more terms are used, for instance, the error reduces by another 5% only with the inclusion of 100 modes. Second, the flow images at $x = 20D$ is approximated by the eigenfunctions and the results are shown in Fig. 4(a). Instead of considering the mean square error, we consider $1 - \varepsilon_n$ as a measure of turbulence captured by the selected number of modes. The variation of this measure with the number of modes included is shown in Fig. 4(b). It is clear from Fig. 4(b) that turbulence is readily captured up to the inclusion of about 30 modes and thereafter the rate of convergence decreases and the curves level off at 40 or more modes. At this plateau, about 70% of the turbulence field is represented. The same trend is ob served at other x station and the results at $x = 10D$ is shown in Fig. 4(b) for comparison. This demonstration implies that the first 40 modes are enough for representing the gross behavior of flow in

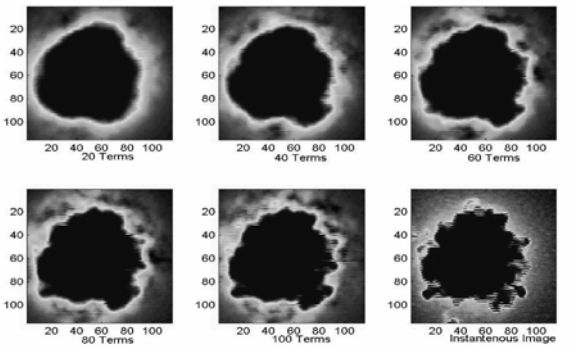

Fig. 3(a) Reconstructed image at x = 10D

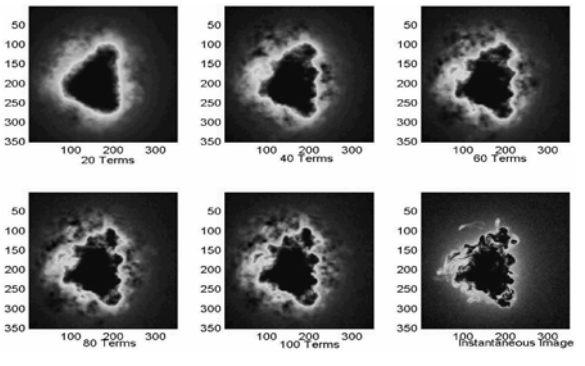

Fig. 3(b) Reconstructed image at x = 30D

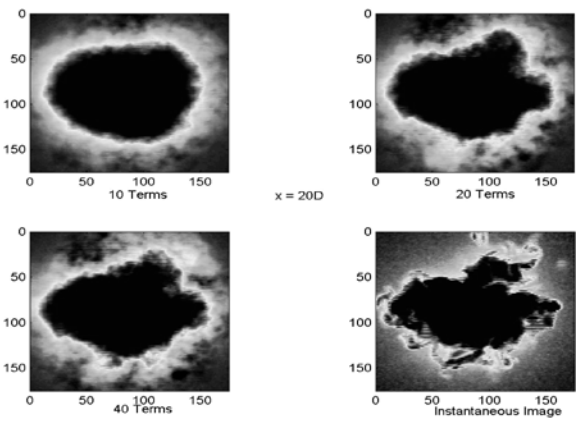

Fig. 4(a) Approximated image at x = 20D

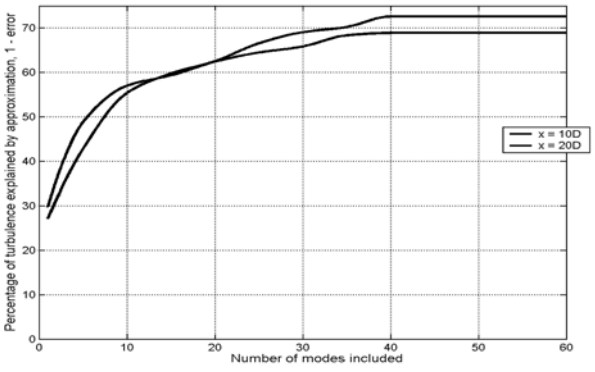

Fig. 4(b) Approximation error curve

approximation; the jet flow is governed by certain dominant eddies that are well captured by shapes of the principal modes. Therefore, we can use combinations of these modes to produce realistic jet representations.

3.2.2 JET IMAGE GENERATIONS WITH SELECTED PRINCIPLE MODES

It is hypothesized that a_k / λ_k are generated randomly and uniformly over the range of (−1, 1) and by doing so we can obtain jet realization in a time sequence of any lengths. As described above, the first 40 principal modes are sufficient to produce satisfactory flow images and hence they are used for random generation of flow images at all jet sections. The results of five examples of flow images generated at the section $x = 10D$ are shown in Fig. 5. The corresponding experimentally measured images are shown and the comparison is good. In addition, the time-averaged LIF image of mean concentration field in the experiment can also be recovered from the randomly generated sequence of LIF images. This assures the validity of the proposed scheme.

3.3 JET FLOW FIELD ON LONGITUDINAL SECTION

Instantaneous flow field on the longitudinal section of the jet, through the jet centerline, can be obtained from the information at all jet sections. Flow images are reconstructed and approximated at jet sections spanning from $x = 10D$ to $60D$, with intervals at $1D$. The average flow field is calculated from the instantaneous images and compared to the analytical solution of a co-flow momentum jet (Lee and Chu 2003)

$$U^{*2} + U^{*} - \frac{1}{\pi B^{*2}} = 0 \; ; \qquad \frac{dB^{*}}{dx^{*}} = \beta_s \frac{U^{*}}{1+U^{*}}$$

where $U^{*} = \Delta U / U_a$, $B^{*} = B / l_m^{*}$ and $x^{*} = x / l_m^{*}$. ΔU is the excess velocity; $l_m^{*} = M_e^{1/2} / U_a$ is the excess momentum length scale; $B = \sqrt{2} b_{gc}$ is the top-hat concentration half width. Comparison of the flow field is shown in Fig. 6 via the downstream development of the concentration jet width. It is evident that the linear interpolation scheme works satisfactorily, at least in reproducing the correct trend of jet width development.

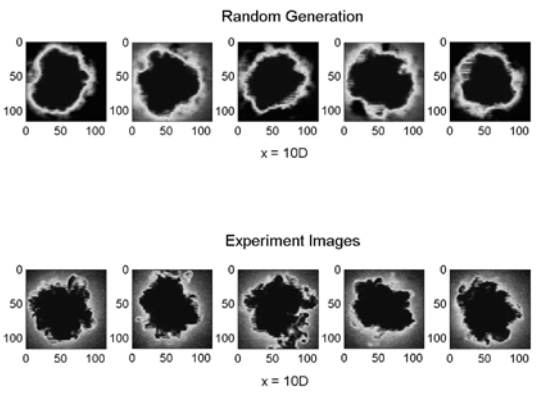

Fig. 5 Randomly generated image at x = 10D

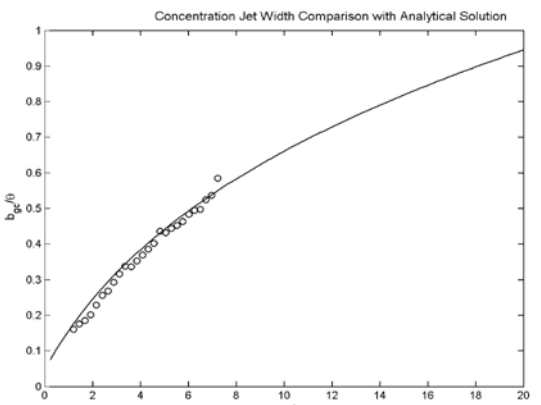

Fig. 6 Concentration jet width (θ means l_m^{*})

4 CONCLUSION

An approach is presented for virtual construction of turbulent jet flow images at extended spatial and temporal locations from a database of experimental data at limited spatial stations. The approach, based on flow field representation and reconstruction using the POD, is applied to LIF images of a coflowing jet. It is observed that the gross shapes of the principal modes do not depend strongly on the ensemble size. This implies that the flow is characterized by dominant eddies of lower orders (modes) which govern the main flow mechanics. Furthermore, we found that these principal modes remain essentially unchanged between any two adjacent measurement stations. This observation enables us to apply the linear interpolation scheme for the

approximation of flow images at an intermediate station. The proposed reconstruction and approximation of flow images are validated through a close agreement of jet concentration width between the constructed images and the analytical solution.

ACKNOWLEDGMENT

The investigation is supported by a research grant (HKU 7517/03E) awarded by the Research Grants Council of Hong Kong.

REFERENCES

Baumgartner DJ, Frick WE, Fox CG (1994) Improved prediction of bending plumes. Journal of Hydraulic Research 32: 935-950

Bernero S, Fiedler HE (2000) Application of particle image velocimetry and proper orthogonal decomposition to the study of a jet in a counterflow. Exp. Fluids 29: 274-281

Glauser MN, Leib SJ, George WK (1987) Coherent structures in the axisymmetric turbulent jet mixing layer. In: Turbulent Shear Flow 5: 134-145. Springer-Verlag, New York

Holmes P, Lumley JL, Berkooz G (1999) Turbulence, Coherent Structures, Dynamical Systems and Symmetery. Cambridge University Press, Cambridge

Lee JHW, Chu VH (2003) Turbulent jets and plume: a Lagrangian approach. Kluwer Academic Publishers, the Netherlands